ISTITUTO NAZIONALE DI FISICA NUCLEARE
Laboratori Nazionali di Frascati

LNF-83/99

M. De Crescenzi et al. : TEMPERATURE INDUCED ASYMMETRIC EFFECTS IN THE SURFACE EXTENDED ENERGY LOSS FINE STRUCTURE OF Ni(100)

Estratto da:
Solid State Comm. 46, 875 (1983)

Servizio Documentazione
dei Laboratori Nazionali di Frascati
Cas. Postale 13 - Frascati (Roma)

Solid State Communications, Vol. 46, No. 12, pp. 875–880, 1983.
Printed in Great Britain.

0038–1098/83 $3.00 + .00
Pergamon Press Ltd.

TEMPERATURE INDUCED ASYMMETRIC EFFECTS IN THE SURFACE EXTENDED ENERGY LOSS FINE STRUCTURE OF Ni(1 0 0)

M. De Crescenzi

Dipartimento di Fisica, Università della Calabria, Cosenza, Italy

F. Antonangeli and C. Bellini

Gruppo PULS, Laboratori Nazionali di Frascati, Frascati, Italy

and

R. Rosei

Istituto di Fisica, Università di Trieste, Trieste, Italy

(*Received* 10 *January* 1983 *by F. Bassani*)

Electron energy loss spectra have been detected on a Ni(1 0 0) surface above the $M_{2,3}$ core edge at several different temperatures, between 80 and 1300 K. We find a strong temperature dependence of the SEELFS signal. In particular we find a strong attenuation of the signal on increasing the temperature (especially the part originating from higher coordination shells). We find also an *apparent* contraction of the nearest neighbour distance obtained by the Fourier transform technique. We present a model calculation by which we tentatively interpret the apparent contraction as originating from an artifact introduced by the experimental integration limits of the Fourier transform. This in turn is due to an asymmetric pair distribution function of atoms in the surface region.

1. INTRODUCTION

IN THE LAST YEAR a new technique for surface structural determinations has been presented [1–3], which usefully complements the established methods of investigation (LEED [4, 5], SEXAFS [6–8], NPD [9] and EAPFS [10, 11] etc.). The technique relies on the detection of fine structures in the reflection electron energy loss spectra, recorded above a core-level edge. For this reason it was termed SEELFS (Surface Extended Energy Loss Fine Structure). Results on bulk solids (Cu and Ni [1, 2], Fe [12], Pd [13], Ru [14] and Graphite [15]), and absorbates (O_2/Al [16], O_2/Ni(1 0 0) [17], C/Ni(1 1 1) [18]), have shown that SEELFS is a reliable technique, very simple to use, and its experimental results are easy to analyze.

Indeed the surface sensitivity of the method was shown to be exceedingly good, permitting structural determination of adsorbates in submonolayer quantities without undue efforts [17, 18]. Working with a current of just a few μA, the signal to noise ratio is also much better than obtainable with SEXAFS, even at the highest photon fluxes currently available in the 100–1000 eV photon energy range [7] (using the same data acquisition times).

The experimental simplicity of the technique allows one to extend the measurements in several directions (which have not been attempted with SEXAFS so far). So, for instance, it has been possible to investigate the behaviour of the atoms of the substrate [17, 18] upon adsorption of a surface species.

In the following we report on the temperature dependence of the EELFS oscillations above the $M_{2,3}$ core-levels of a Ni(1 0 0) surface up to 1300 K. Rather surprisingly, we find an *apparent* contraction with the temperature of the lattice parameter (instead than the expected thermal expansion). We present a tentative interpretation of this effect as originating from the strong anharmonic contribution in the atomic pair potential in the surface region.

A similar effect has been already detected in EXAFS spectra of various compounds (e.g. Zn [19, 20], superionic conductors [21], etc.) but it is the first time, to our knowledge, that it is seen on a surface.

We find also that at high temperature the EXAFS-like oscillations are strongly attenuated. The first nearest-neighbour peak in the radial distribution function is, however, always present, while the contribution of the outer shells progressively disappear in noise in the higher temperature spectra.

We finally present a simple model which allows us to extract an evaluation of several parameters of the surface pair distribution function.

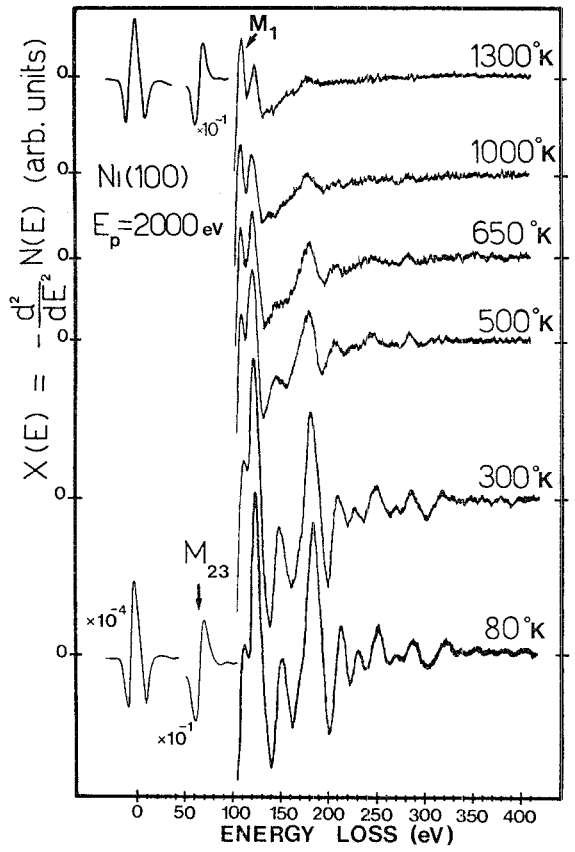

Fig. 1. Extended Energy Loss Fine Structure (EELFS) spectra above the Ni(1 0 0) $M_{2,3}$ core-level as a function of temperature (80–1300 K). The primary beam energy was E_p = 2000 eV. The spectra were all recorded with the same experimental settings.

2. EXPERIMENTAL

A commercial Varian chamber equipped with a single pass Cylindrical Mirror Analyzer ($\Delta E/E = 0.4\%$) was used for the experiments. A nickel single crystal was cut to expose a (1 0 0) face (within 1°). The sample was mechanically polished and chemically etched using standard procedures and mounted on a $XYZ\theta$ manipulator. The *in situ* cleaning was accomplished by cycles of argon ion-sputtering (2 keV, 10 min and 10^{-6} torr) and heating at 1000°C.

Oxidation and reduction cycles were also used for eliminating residual carbon. The cleanliness of the surface was checked by Auger spectroscopy and LEED. The crystal temperature could be varied between 80 K (by flowing liquid nitrogen in the feedthrough) to 1300 K by heating of the sample holder. The temperature was measured by an iron–constantane thermocouple spot-welded on the edge of the sample. The high temperature thermocouple calibration was checked with an optical pyrometer. The CMA was operated with

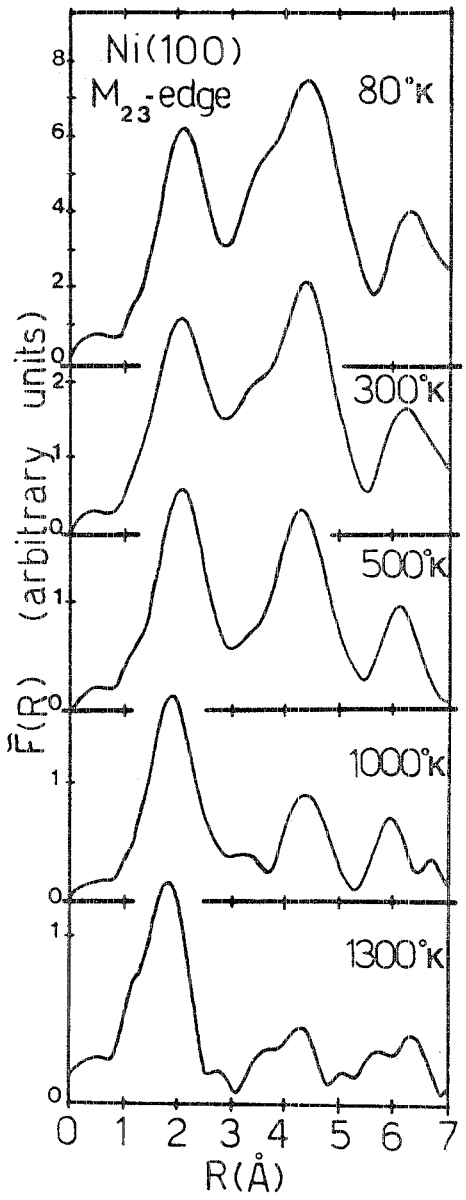

Fig. 2. Fourier transforms $\tilde{F}(R)$ of the EELFS signals of Fig. 1. The integration limits were k_{min} = 3.0 Å^{-1} and k_{max} = 10.0 Å^{-1} for all spectra.

5–10 V modulation voltages in the second derivative mode.

Primary electron energies between 1000 and 2000 eV and currents of ~ 5 μA were used. Typical acquisition times for a single run at a given temperature were 15 min.

Other experimental details can be obtained from [1].

We would like to emphasize here that the basic requirements experimental set-ups of the SEELFS technique are identical to those of the Auger spectroscopy.

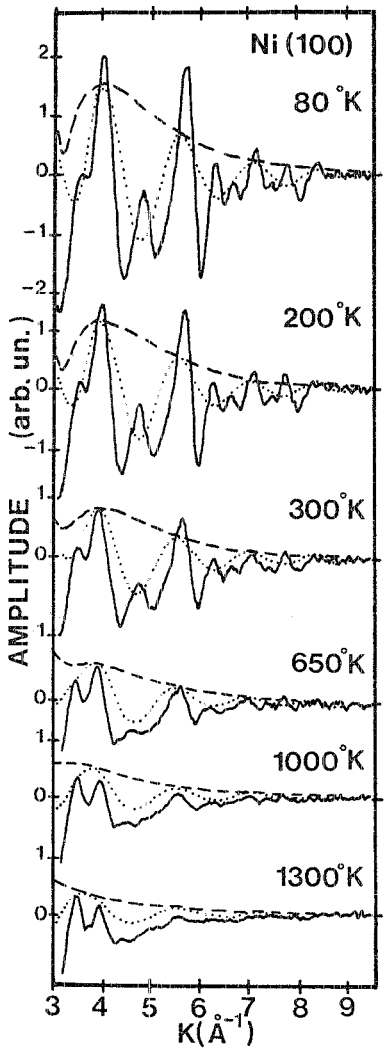

Fig. 3. Solid line: experimental function $X(K)$ of the EELFS signals above the Ni $M_{2,3}$ core-level at different temperatures. Dotted line: back-Fourier transform contribution of the nearest neighbours distance. Dashed line: backscattering amplitude.

3. EXPERIMENTAL RESULTS AND DISCUSSION

Figure 1 shows SEELFS spectra of the Ni(1 0 0) surface for many different temperatures, taken with a primary beam energy of 2000 eV. Identical experimental settings were used for recording all the spectra.

The atomic features ($M_{2,3}$ and M_1 edges) remain substantially unchanged on increasing the temperature. In comparison, the EXAFS-like structure which extend for about 350 eV above the $M_{2,3}$ edge, are progressively attenuated. At 1300 K the structural information becomes much weaker than the M_1 atomic feature.

Extended fine structures in the reflection energy loss spectra may be analyzed with the same procedure of the EXAFS spectra. Structural information around each atom can be obtained from the oscillatory part

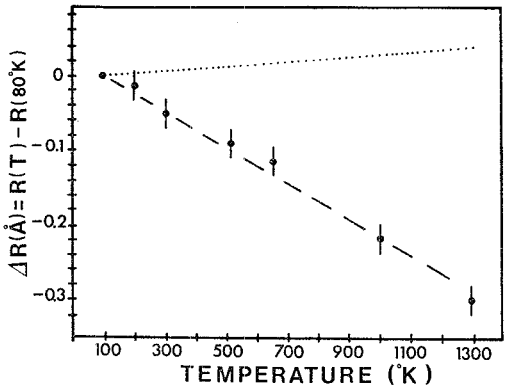

Fig. 4. Temperature dependence of the differential nearest neighbour distance $\Delta R(\text{Å}) = R(T) - R\,(80\,\text{K})$ determined from the position of the peak of $\tilde{F}(R)$. The dotted line is the estimated ΔR(Å) from the thermal expansion coefficient of [27].

of $X(E) = -(\mathrm{d}^2/\mathrm{d}E^2)N(E)$ via the Fourier transform [22]:

$$\tilde{F}(R) = \frac{1}{\sqrt{2\pi}} \int_{k_{\max}}^{k_{\min}} X(K)\, K^n W(K)\, \mathrm{e}^{-2iKR}\, \mathrm{d}K, \qquad (1)$$

where K is the photoelectron wavevector ($K(\text{Å}^{-1}) = \sqrt{0.263(E - E_0)}\,\text{eV}$, E_0 is the edge onset), K^n is an appropriate weight factor and $W(K)$ is a window function to avoid truncation effects on $X(K)$.

Figure 2 shows the Fourier transforms of the SEELFS spectra obtained by always using the identical k-range integration ($K_{\min} = 3.0\,\text{Å}^{-1}$ and $K_{\max} = 10.0\,\text{Å}^{-1}$).

The temperature has a very dramatic effect on the peaks due to the higher coordination shells. They rapidly decrease upon increasing the temperature and disappear below the noise level at the highest temperature of the experiment. This effect should be expected from an EXAFS-like signal since the disorder introduced by temperature is most effective in destroying the correlation [23, 24] of the outer shells.

It is important to note that this finding proves beyond reasonable doubt the structural origin of the fine structures in our spectra. It also rules out the possibility of sizeable contributions from plasmon replicas [25, 26] to the spectra which would appear in the low K region of the spectrum and would be only slightly temperature dependent. Fig. 3 shows the effect of temperature on the backscattering amplitude. On going from 80 to 1300 K, besides the progressive attenuation, we note a shift of the curve (dashed line) towards lower K values.

The most dramatic effect in the $F(R)$ spectra, however, on increasing the temperature, is a marked shift (~ 0.25 Å) of the first peak towards *lower* R values. The temperature dependence of the nearest neighbour

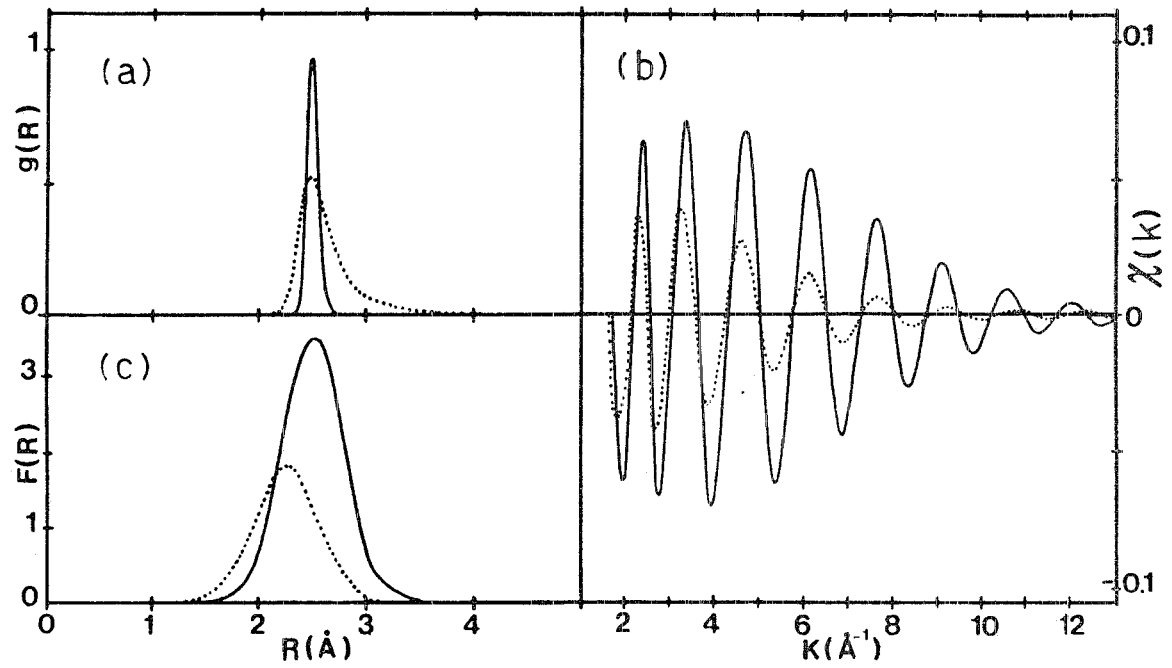

Fig. 5. (a) Model calculation of the pair distribution function $g(R) = e^{-U(R)/kT}$ for two different temperatures; (solid line: 80 K, dotted line: 1000 K). $U(R)$ is a Morse pair potential for Ni calculated as described in [34]. (b) EXAFS $\chi(K)$ (from equation 2) computed with the two $g(R)$ shown in (a). (c) Fourier transforms of the EXAFS functions of (b) between 3.0 and 12 Å^{-1}. The total phase shift $\Phi_{tot}(K)$ of equation 2 was taken equal to zero in *both* cases in order to emphasize the apparent contraction of the lattice parameter (see dotted curve) due to the asymmetry of $g(R)$.

distance of Ni atoms on the (1 0 0) surface is shown in Fig. 4. Also reported is the expected dependence obtained from bulk thermal expansion data [27].

This apparent contraction of the radial distribution function is certainly non-physical. We propose that it might be interpreted as an effect related to asymmetric pair distribution functions originating from anharmonic contributions to the surface pair potential.

As mentioned before, similar effects have been detected in EXAFS experiments on bulk samples in cases in which the assumption of a Gaussian pair distribution fails (e.g. solid [19] and liquid [20] Zn, superionic conductors [21] etc.).

Conventional EXAFS spectra [28] above the K-edge of a 10 μm thick nickel film in the 80–600 K range behaves as expected, showing, on increasing the temperature, only a broadening in the $F(R)$ structures (originating from an increased Debye–Waller factor [24]). *No shift* of the nearest neighbour distance was detected (within 0.02 Å) in this case. Similar results were obtained on Cu bulk samples [23, 29].

The apparent shift of the nearest neighbours peak in the SEELFS experiments is therefore peculiar of the surface region sampled by our technique. The enhanced anharmonic contribution in the interatomic potential energy curve in the surface region and the wider surface atomic vibrations [31, 32] could therefore be responsible for the observed effect.

In order to test this assumption we have implemented a simple model along the lines of [19] and [20].

The EXAFS interference function $\chi(K)$ can be written as:

$$\chi(K) = \int g(R) \frac{e^{-2R/\lambda}}{KR^2} A(K,\pi) \sin[2KR + \Phi_{tot}(K)]\, dR, \tag{2}$$

where $g(R)$ is the pair radial distribution function. Assuming a Morse potential of the form [33, 34]:

$$U(R) = D\{e^{-2\alpha(R-R_0)} - 2e^{-\alpha(R-R_0)}\}, \tag{3}$$

$g(R)$ can be written as:

$$g(R) = e^{-U(R)/kT}. \tag{4}$$

By introducing the $g(R)$ calculated for $T = 80$ and $T = 1000$ K are shown in Fig. 5(a) as a solid line and a dashed line respectively. The effect of the asymmetric $g(R)$ is apparent in Fig. 5(c). The distribution at low temperature gives an $F(R)$ correctly peaked at the nearest neighbour distance assumed in the model. The asymmetric high temperature $g(R)$ gives rise to (still with a phase shift $\Phi_{tot}(K) = 0$) an $F(R)$ displaced by 0.20 Å.

The effect of the asymmetric $g(R)$ can be better understood from Fig. 5(b) which shows the function $\chi(K)$ calculated in the two cases. The period of the function $\chi(K)$ (solid line) originating from the symmetric $g(R)$ is constant through the spectrum. The function $\chi(K)$ for the high temperature, on the other hand, has a variable period. As noted by Eisenberger and Brown [19], the information contained in the sharp rise of the asymmetric $g(R)$ will manifest itself at high K, while the information contained in the tail will be present only at small K's. This last contribution is unavoidably lost in performing the Fourier transform in the typical experimentally usable region ($k_{\min} \cong 3.0$ Å^{-1} and $k_{\max} \cong 12.0$ Å^{-1}).

The EXAFS-like spectroscopies (EXAFS, SEXAFS, NPD, EAPFS and SEELFS) which weight the high K region of the spectrum will therefore detect an (apparent) contraction at high temperature. LEED spectroscopy which instead is sensitive to the low K region will detect an increase of the average pair distribution function [36]. We suspect that strong anharmonic effects may be present as a rule on surface. Surface nearest neighbours distances determined with EXAFS-like spectroscopies at room temperature may therefore be affected. Some of the discrepancies in the literature between LEED and SEXAFS results may, at least in part, originate from this effect.

In conclusion, we have shown in this communication a strong dependence of the EXAFS-like signal detected above the $M_{2,3}$ core-edge of a Ni(1 0 0) surface by SEELFS spectroscopy. The attenuation of the signal with temperature was expected and proves beyond reasonable doubt its EXAFS origin. The unexpected apparent contraction detected in the experiment has been tentatively interpreted as originating from the asymmetric pair distribution function in the surface region (which affects the nearest neighbour distance determination obtained through the Fourier transform technique). We have also provided new convincing evidence of the usefulness and flexibility of the new SEELFS technique.

REFERENCES

1. M. De Crescenzi, L. Papagno, G. Chiarello, R. Scarmozzino, E. Colavita, R. Rosei & S. Mobilio, *Solid State Commun.* **40**, 613 (1981).
2. L. Papagno, M. De Crescenzi, G. Chiarello, E. Colavita, L.S. Caputi & R. Rosei, *Surf. Sci.* **117**, 525 (1982).
3. M. De Crescenzi, *Proc. of Int. Conf. on 'EXAFS and Near Edge Structures'*, Frascati, 13–18 September, Springer-Verlag (1982) (in press).
4. F. Jona, *J. Phys.* **C11**, 4271 (1978) (and references therein).
5. J.E. Demuth, D.W. Jepsen & P.M. Marcus, *Phys. Rev.* **B11**, 1460 (1975).
6. P.H. Citrin, P. Eisenberger & R.C. Hewitt, *Phys. Rev. Lett.* **41**, 309 (1978).
7. J. Stöhr, L.I. Johansson, I. Lindau & P. Pianetta, *Phys. Rev.* **B20**, 664 (1979).
8. J. Stöhr, L.I. Johansson, S. Brennan, M. Hecht & J.N. Miller, *Phys. Rev.* **B22**, 4052 (1980).
9. D.H. Rosenblatt, J.G. Tobin, M.G. Mason, R.F. Davis, S.D. Kevan, D.A. Shirley, C.H. Li & S.Y. Tong, *Phys. Rev.* **B23**, 3828 (1981) (and references therein).
10. M.L. den Boer, T.L. Einstein, W.T. Elam, R.L. Park, L.D. Roelofs & G.E. Laramore, *Phys. Rev. Lett.* **44**, 496 (1980).
11. M.L. den Boer, T.L. Einstein, W.T. Elam, R.L. Park, L.D. Roelofs & G.E. Laramore, *J. Vac. Sci. Technol.* **17**, 59 (1980).
12. S. Polizzi, F. Antonangeli, G. Chiarello & M. De Crescenzi (to be published).
13. G. Chiarello, E. Colavita, M. De Crescenzi & S. Nannarone (to be published).
14. L. Papagno, L.S. Caputi, F. Ciccacci & C. Mariani (to be published).
15. L. Papagno, L.S. Caputi, M. De Crescenzi & R. Rosei, *Phys. Rev.* **B26**, 2320 (1982).
16. M. De Crescenzi, G. Chiarello, E. Colavita & R. Rosei, *Solid State Commun.* **44**, 845 (1982).
17. M. De Crescenzi, F. Antonangeli, C. Bellini & R. Rosei, *Phys. Rev. Lett.* (in press).
18. R. Rosei, M. De Crescenzi, S. Modesti, F. Sette, C. Quaresima, A. Savoia & P. Perfetti *Phys. Rev. B* (in press).
19. P. Eisenberger & G.S. Brown, *Solid State Commun.* **29**, 481 (1979).
20. E.D. Crozier & A.J. Seary, *Canad. J. Phys.* **58**, 1388 (1980); E.D. Crozier, *EXAFS Spectroscopy* (Edited by B.K. Teo & D.C. Joy), p. 89. Plenum Press, New York (1981).
21. J.B. Boyce, T.M. Hayes, J.C. Mikkelsen, Jr. & W. Stutius, *Solid State Commun.* **33**, 183 (1980); J.B. Boyce, T.M. Hayes & J.C. Mikkelsen, Jr., *Phys. Rev.* **B23**, 2876 (1981) (and references therein).
22. The symbol $\tilde{F}(R)$ was chosen as a reminder that the procedure of the Fourier-transforming the second derivative of the spectra gives a function $\tilde{F}(R) \propto R^2 F(R)$ where $F(R)$ is the usual EXAFS radial distribution function.
23. R.B. Greegor & F.W. Lytle, *Phys. Rev.* **B20**, 4902 (1979).
24. E. Sevillano, H. Meuth & J.J. Rehr, *Phys. Rev.* **B20**, 4908 (1979).
25. Plasmon replicas are however important in free electron-like metals (see [12, 26]).
26. P.M.Th.M. van Attekum & J.M. Trooster, *Phys. Rev.* **B18**, 3872 (1978).
27. W.B. Pearson, *Handbook of Lattice Spacing and Structures of Metals and Alloys*, Pergamon Press, New York (1958).
28. M. De Crescenzi (to be published).
29. W. Böhmer & P. Rabe, *J. Phys.* **C12**, 2465 (1979).
30. We estimate a sampling depth of 10–15 Å depending on the primary electron energy used in the experiment.
31. B.C. Clark, R. Herman & R.F. Wallis, *Phys. Rev.* **139**, A860 (1965).
32. G. Ertl & J. Küppers, *Low Energy Electrons*

and Surface Chemistry, Ch. 10, p. 193. Verlag Chemie (1974) (and references therein).
33. D.P. Jackson, *Surf. Sci.* **43**, 431 (1974).
34. L.A. Girifalco & V.G. Weizer, *Phys. Rev.* **114**, 687 (1959).
35. S.D. Kevan, J.G. Tobin, D.H. Rosenblatt, R.F. Davis & D.A. Shirley, *Phys. Rev.* **B23**, 493 (1981).
36. P.E. Vilijoen, B.J. Wessels, G.L.P. Berning & J.P. Roux, *J. Vac. Sci. Technol.* **20**, 204 (1982).